Review Article

Xiaohui Zhang, Yi Zhang*, Baohong Tian*, Kexing Song*, Ping Liu*, Yanlin Jia*, Xiaohong Chen, Junchao An, Zhuan Zhao, Yong Liu, Alex A. Volinsky, Xu Li, and Ting Yin

Review of nano-phase effects in high strength and conductivity copper alloys

https://doi.org/10.1515/ntrev-2019-0034
Received Aug 03, 2019; accepted Aug 22, 2019

Abstract: Copper alloys and copper matrix composites have been attracting a lot of attention lately. Their composition design, preparation, and processing directly affect the final performance. In this review, several typical copper alloys, such as Cu-Fe-P, Cu-Ni-Si, and Cu-Cr-Zr are analyzed. The deformation mechanisms, microstructure evolution, and dynamic recrystallization behavior are summarized. In addition, dispersion strengthened copper matrix composites and graphene reinforced copper matrix composites are reviewed.

1 Introduction

Owing to its high electrical and thermal conductivity, along with remarkable processing performance, copper is widely used in the aerospace and electronics industries, including high-speed rail contact wires and electrical contact materials [1–3], as shown in Figure 1. However, the strength of pure copper is low at room and high temperatures. Although the strength increases significantly

Figure 1: The emerging applications of copper alloys.

***Corresponding Author: Yi Zhang:** School of Materials Science and Engineering, Henan University of Science and Technology, Luoyang 471023, China; Collaborative Innovation Center of Nonferrous Metals, Henan Province, Luoyang 471023, China; Henan Key Laboratory of Nonferrous Materials Science and Processing Technology, Luoyang 471023, China; Email: zhshgu436@163.com
***Corresponding Author: Baohong Tian:** School of Materials Science and Engineering, Henan University of Science and Technology, Luoyang 471023, China; Collaborative Innovation Center of Nonferrous Metals, Henan Province, Luoyang 471023, China; Henan Key Laboratory of Nonferrous Materials Science and Processing Technology, Luoyang 471023, China; Email: bhtian007@163.com
***Corresponding Author: Kexing Song:** School of Materials Science and Engineering, Henan University of Science and Technology, Luoyang 471023, China; Collaborative Innovation Center of Nonferrous Metals, Henan Province, Luoyang 471023, China; Henan Key Laboratory of Nonferrous Materials Science and Processing Technology, Luoyang 471023, China; Email: kxsong123@163.com
***Corresponding Author: Ping Liu:** School of Materials Science and Engineering, University of Shanghai for Science and Technology, Shanghai 200093, China; Email: liuping@usst.edu.cn
***Corresponding Author: Yanlin Jia:** College of Materials Science and Engineering, Beijing University of Technology, Beijing 100124, China; Email: jiayanlin@126.com
Xiaohui Zhang, Zhuan Zhao, Yong Liu, Ting Yin: School of Materials Science and Engineering, Henan University of Science and Technology, Luoyang 471023, China; Collaborative Innovation Center of Nonferrous Metals, Henan Province, Luoyang 471023, China; Henan Key Laboratory of Nonferrous Materials Science and Processing Technology, Luoyang 471023, China
Xiaohui Zhang and **Yi Zhang** contributed equally to this work
Xiaohong Chen: School of Materials Science and Engineering, University of Shanghai for Science and Technology, Shanghai 200093, China
Junchao An: School of Materials Science and Engineering, Luoyang Institute of Science and Technology, Luoyang 471023, China
Alex A. Volinsky: Department of Mechanical Engineering, University of South Florida, Tampa 33620, United States of America
Xu Li: Center for Advanced Measurement Science, National Institute of Metrology, Beijing 100029, China

Open Access. © 2019 X. Zhang *et al.*, published by De Gruyter. CC BY This work is licensed under the Creative Commons Attribution 4.0 License

Unauthenticated
Download Date | 12/11/19 7:47 AM

after cold processing, the elongation is low and the obtained strength is reduced during the annealing process, which seriously restricts the applications of pure copper. Fortunately, copper alloys and copper-based composites prepared through various strengthening mechanisms not only have high electrical and thermal conductivity, but also high strength and plasticity, along with good processing performance [4–9]. Therefore, high strength and high conductivity copper alloys and copper matrix composites have drawn more attention in the past few years.

The methods of strengthening copper alloys include solution strengthening, aging precipitation strengthening and dispersion strengthening. For solution strengthening some alloying elements are dissolved in the copper matrix, which results in lattice distortion and enhances the strength of the alloy by hindering dislocations movement. However, due to the scattering effect of electrons on the solute atoms, the electrical conductivity of the alloy can be severely reduced, thus solution strengthening is often used in conjunction with other strengthening methods [10, 11]. Aging strengthening refers to the addition of elements in the copper matrix whose solid solubility changes greatly at high and room temperatures, such as Cr [12–14], Zr [15, 16], Ni [17, 18], Mg [11, 19], Nb [20, 21] etc. After solution and aging treatment, the secondary phase is formed, thereby improving the strength by preventing dislocations and grain boundaries movement. Krishna *et al.* [22] revealed that the increase of hardness and conductivity during aging was mainly attributed to the formation of fine Ni_2Si and Co_2Si nano-precipitates in the Cu-Ni-Si-Co alloy. Zhang *et al.* [23] investigated the microstructure evolution of the Cu-Ni-Si-P alloy during aging and found that after aging at 450°C for 48 h, nano δ-Ni_2Si phase precipitated. The addition of P could inhibit the coarsening of the precipitated phase. Huang *et al.* [24] analyzed the microstructure of the Cu-0.31Cr-0.21Zr alloy and concluded that the precipitated phase was $Cu_{51}Zr_{14}$. Cheng *et al.* [25] found that good comprehensive performance of the Cu-0.6Cr-0.15Zr-0.05Mg-0.02Si alloy can be obtained after 80% deformation followed by aging at 480°C for 1 h. Consequently, the hardness and electrical conductivity reached 152 HV and 85.5% IACS, respectively. Tian *et al.* [26] reported that the electrical conductivity of the Cu-1.0Zr alloy was 80% IACS and the microhardness reached 155 HV after solution treatment at 900°C for 1 h and aging at 500°C for 1 h. Furthermore, after aging at 450°C for 6 h, a large amount of the $Cu_{10}Zr_7$ phase precipitated in the copper matrix. Dong *et al.* [27] established that the resistance to softening of the Cu-0.7Fe-0.15P alloy was improved after aging due to the precipitation of the Fe_2P phase. In addition to doping common alloying elements, many researchers have tried to add rare earth elements, such as Ce and Y, to obtain good properties. Wang *et al.* [28] investigated the effects of Ce and Y on the hot deformation of the Cu-Mg alloy and reported that rare earth elements can not only refine grains, but also improve the flow stress and thermal activation energy of the alloy. Zhang *et al.* [29] reported that Y can increase the activation energy during the hot deformation of the Cu-Zr alloy, affecting the dynamic recrystallization behavior. Also, Ce can refine the grain of the Cu-0.2Zr alloy and enhance the hot processing stability.

With the rapid development of the high-tech industries, the performance of the traditional copper alloys cannot satisfy the modern requirements. In recent years, some researchers started to gradually pay attention to the copper matrix composites, including oxide, carbide, nitride, boride nano-particles dispersion strengthening copper matrix composites [30–32]. The dispersion strengthening composites can be divided into in-situ reinforced and ex-situ reinforced metal matrix composites. Due to the in-situ formation of the reinforcement phase through metallurgical reactions, chemical catalytic transformations, and plastic deformation, the in-situ reinforcement can enhance the chemical stability and interface compatibility between the reinforcement and the matrix, thus improving the interface bonding and mechanical properties [33–35]. For instance, nano-Al_2O_3 and nano-Cr_2O_3 dispersion strengthened copper alloys fabricated by internal oxidation belong to the in-situ reinforced metal matrix composites. Furthermore, the scattering effect of electrons on solute atoms in the copper matrix is greater than that caused by the secondary phase, so dispersion strengthened copper matrix composites can enhance the material strength while ensuring the electrical conductivity. Bera *et al.* [36] reported that the hardness and wear resistance of the Cu-10Cr-3Ag electrical contact sample increased significantly with the addition of nano-Al_2O_3 particles. Zhang *et al.* [37] fabricated the Al_2O_3-Cu/35W5Cr composite by the vacuum hot-pressing sintering and internal oxidation method. Due to the hindering effect on the dislocations caused by the nano-Al_2O_3 particles, the composite was still in the dynamic recovery stage under the hot deformation condition of 850°C and 0.01 s^{-1} strain rate.

Conventionally, hot processing is often carried out to improve the properties of copper alloys. Therefore, the research of the hot processing of copper alloys plays an important role in the improvement of their properties. In this study, the deformation mechanisms, microstructure evolution and its effects on the alloys' properties, along with dynamic recrystallization and aging precipitation mecha-

Unauthenticated
Download Date | 12/11/19 7:47 AM

nisms of several typical copper alloys and copper-based composites during the thermal processing are reviewed.

2 Nano-phase aging precipitation and thermal deformation

2.1 Cu-Fe-P alloy

Cu-Fe-P alloy is widely used as the lead frame material due to its excellent properties. Its precipitates mainly include Fe, Fe_2P and Fe_3P, and the type of precipitation depends on the ratio of Fe and P content. In general, other alloying elements can be added to further improve the comprehensive properties of the alloy. Xiao *et al.* [38] reported the aging precipitation behavior of the Cu-2.3Fe-0.03P alloy. It was demonstrated that the γ-Fe and Fe_3P phases precipitated in the copper matrix. Wang *et al.* [39] also found that the Fe_3P phase precipitated during aging of the Cu-0.88Fe-0.24P alloy. In addition, Dong *et al.* [40] have demonstrated that cold rolling can transform the precipitates from the γ-Fe phase to α-Fe and re-dissolve the fine precipitates into the Cu matrix. Guo *et al.* [41] found that the doped Re facilitated the precipitation of the γ-Fe and Fe_3P phases. In our previous work, the precipitated phase of the Cu-2.3Fe-0.1Zn-0.1P (C194) alloy was investigated using transmission electron microscopy (TEM). The microstructure is shown in Figure 2. Three different kinds of nanoparticles are in the matrix seen in Figure 2(a). First, coarse particles were formed with ellipsoidal shape. Second, the volume of the spherical particles increased to a quarter of the large particles. Third, many small particles dispersed unevenly in the matrix. Figure 2(b) shows the selected electron diffraction pattern (SADP) of the ellipsoid particle. It was demonstrated that the large particle was γ-Fe. Furthermore, the selected electron diffraction pattern in Figure 2(c) and Figure 2(d) confirmed that the α-Fe and Fe_3P nanoparticles precipitated in the matrix. They are corresponding to the "II" and "III" types in Figure 2(a). Furthermore, Cao *et al.* [42] reported that fine γ-Fe and coarse Fe_3P particles were formed in the as-cast Cu-Fe-P alloy. However, the fine Fe particles were dispersed in the interior of the grains due to the process of equal channel angular pressing (ECAP), and the Fe_3P particles pinned the grain boundaries.

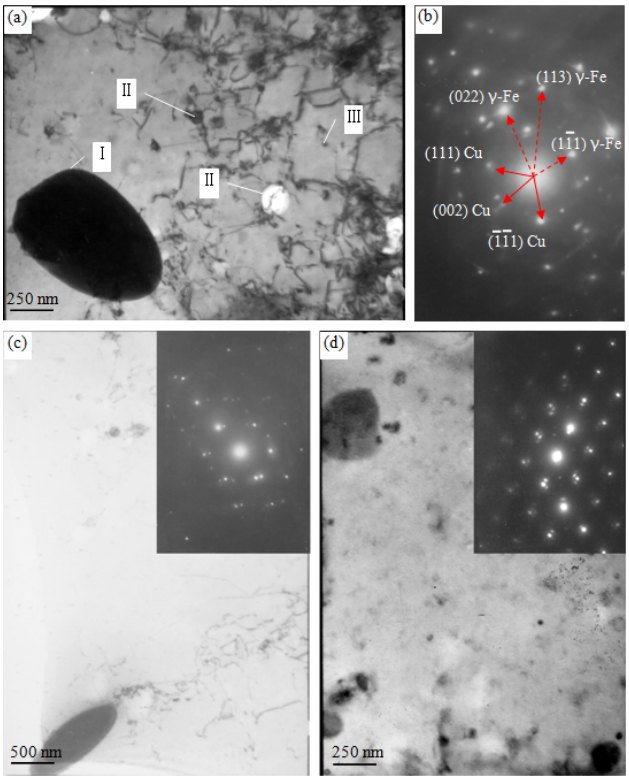

Figure 2: TEM images of the Cu-2.3Fe-0.1Zn-0.1P alloy: (a, c, d) TEM images; (b) SADP image of (a).

2.2 Cu-Ni-Si alloy

Lead frame copper alloy, as the current carrier of the integrated circuits, is a crucial basic material used in the electronics industry. The strength and conductivity of the lead frame material mainly depend on the precipitation strengthening [43]. In general, the strengthening effect depends on the following aspects: the ultimate solubility of alloying elements in copper, the solubility at room temperature, the number and size of precipitates and other factors.

Cu-Ni-Si alloy is widely used as the lead frame material. Ni, Si, and other alloying elements can precipitate into the strengthening phase through aging. Hence, the alloy has high strength and hardness, while the electrical conductivity cannot drop sharply. Wang *et al.* [44] demonstrated that the Cr_3Si and Ni_2SiZr intermediate compounds were formed in the Cu-Ni-Si-Cr-Zr alloy after aging and confirmed that the δ-Ni_2Si phase strengthened the copper matrix through the Orowan mechanism. Hu *et al.* [45] investigated the precipitation and microstructure evolution behavior of the Cu-Ni-Si alloy during hot deformation by means of the high-resolution transmission electron microscopy and first principles calculations and confirmed the precipitation of the δ-Ni_2Si phase. However, in

Unauthenticated
Download Date | 12/11/19 7:47 AM

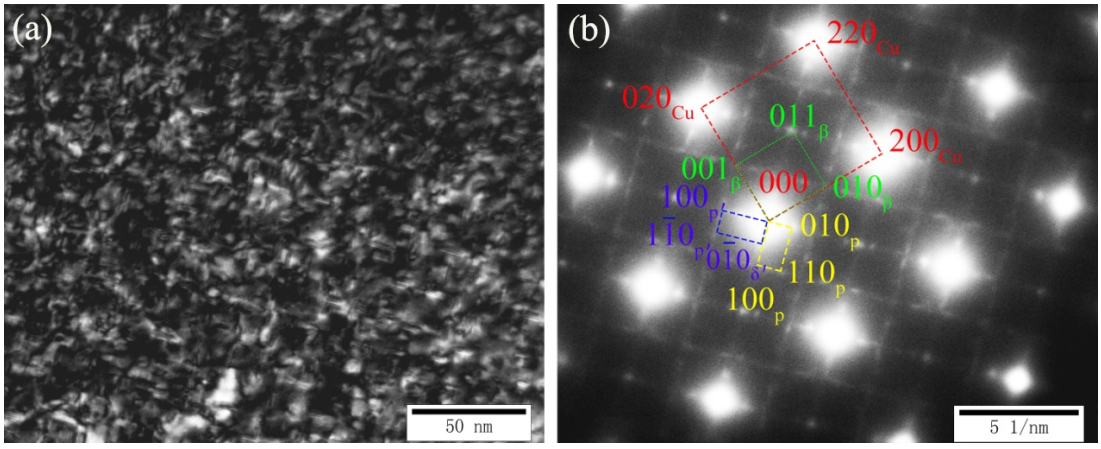

Figure 3: (a) The dark field TEM image of the (Ni, Co)$_2$Si phase and (b) Selected area electron diffraction pattern and indexing.

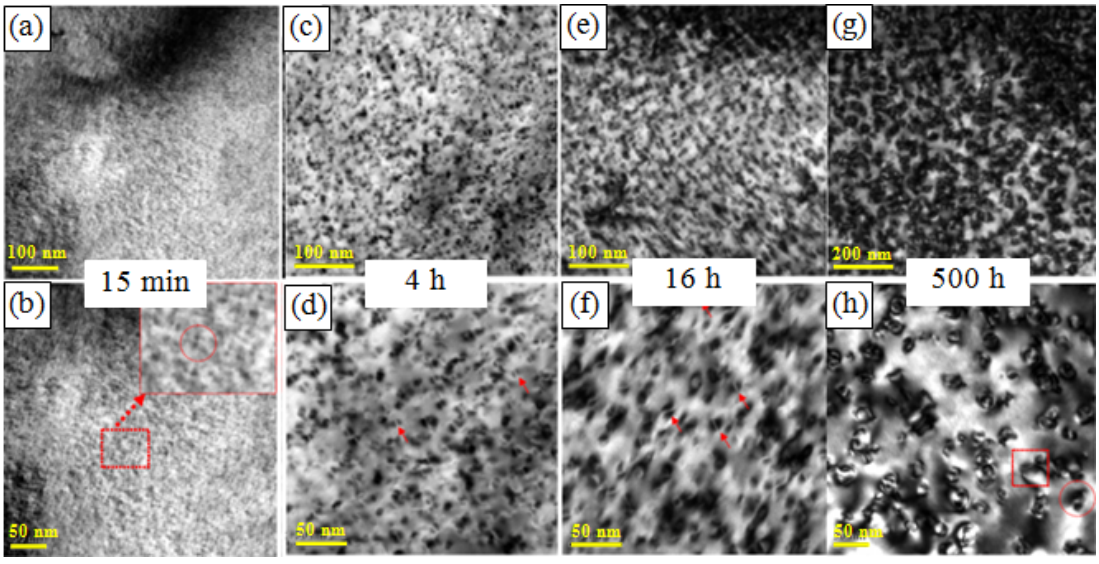

Figure 4: TEM images of the Cu-1.5Ni-0.34Si alloy aged at 450°C for different time: (a, b) 15 min; (c, d) 4 h; (e, f) 16 h; (g, h) 500 h.

the two stages before and after aging, the precipitated δ_1 and δ_2 phases exist, and have different orientations with the copper substrate. Jia *et al.* [46] also confirmed the δ-Ni$_2$Si phase during the aging process of the Cu-3.0Ni-0.72Si alloy, while a layer of metastable δ'-(Cu, Ni)$_2$Si existed around the core. Xiao *et al.* [47] showed that the spinodal decomposition of the precipitated phase was inhibited by doping Co into the Cu-Ni-Si alloy, thus improving the microhardness and conductivity of the alloy. Zhao *et al.* [48] also studied the effects of Co on the microstructure and properties of the Cu-Ni-Si alloy during aging. In addition to the common δ-Ni$_2$Si and β-Ni$_3$Si precipitates, the (Ni, Co)$_2$Si phase was also found, shown in Figure 3. Lei *et al.* [49] systematically investigated the aging precipitation behavior of the Cu-6.0Ni-1.0Si-0.5Al-0.15Mg-0.1Cr alloy and confirmed that the Ni$_2$Si/γ'-Ni$_3$Al and β-Ni$_3$Si precipitation phases cause strengthening effects.

In the present work, the aging precipitation behavior of the Cu-1.5Ni-0.34 Si alloy was investigated at 450°C, and the precipitation coarsening process was analyzed by TEM, as shown in Figure 4.

Figure 4 is similar to the modulated structure at the early aging stage, and then the nanometer precipitation phase gradually appears. Furthermore, the nanoparticles gradually coarsened with the aging time. The size of the precipitates is about 5 nm underaged, 10 nm of the peak aged, and 30 nm overaged. The selected area electron diffraction pattern is shown in Figure 5. In Figure 5 the spinodal decomposition cannot be observed from the SADPs. In addition, the diffraction spots intensified with the aging process. However, the precipitates remained un-

Unauthenticated
Download Date | 12/11/19 7:47 AM

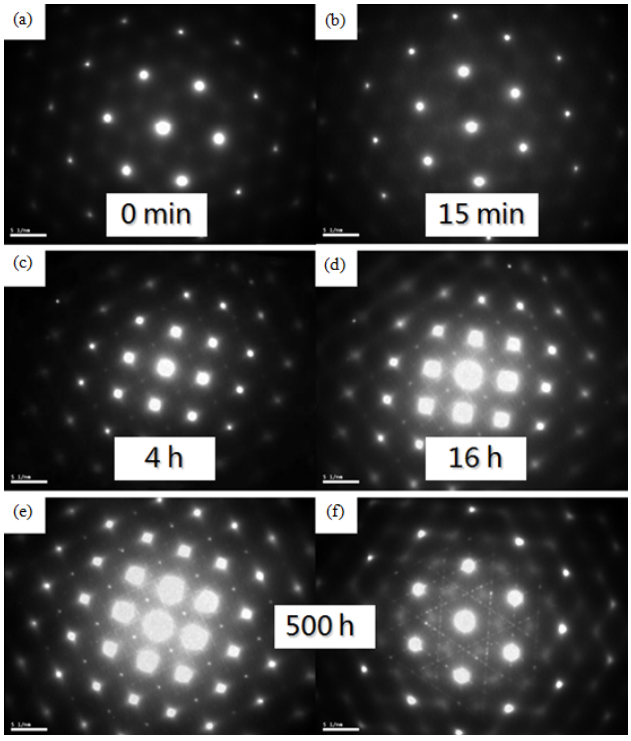

Figure 5: Selected area electron diffraction patterns of the Cu-1.5Ni-0.34Si alloy aged at 450°C for different time: (a) 0 min; (b) 15 min; (c) 4 h; (d) 16 h; (e, f) 500 h.

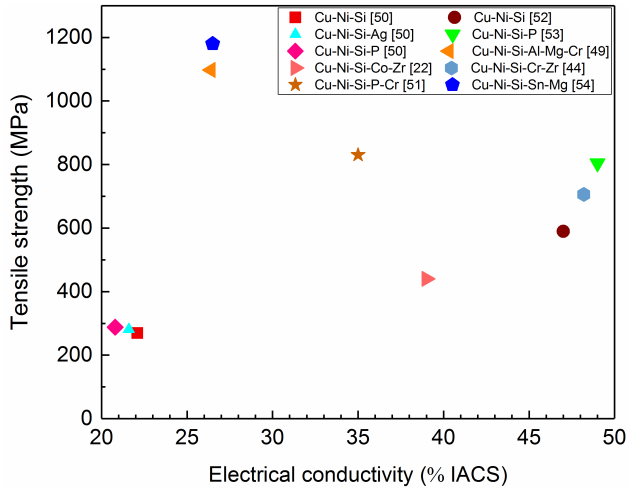

Figure 6: The comprehensive properties of the Cu-Ni-Si alloy doped with different types of alloy elements.

altered. Consequently, Figure 6 shows the comprehensive properties of the Cu-Ni-Si alloy doped with different types of alloying elements.

The aging strengthening and deformation strengthening are often combined in the strengthening treatment of copper alloys. Plastic deformation is the primary method of preparation, processing, and shaping copper alloys. At high temperature copper alloys have low plastic resistance, strong atomic activity, and fast diffusion, which are beneficial for the microstructure improvement and shape forming when accompanied by complete recrystallization. The scientific and practical formulation of hot deformation parameters for copper alloys is of great significance to their quality and performance. Zhang *et al.* [55] studied the hot deformation behavior of the Cu-2Ni-0.5Si alloy at 600-800°C and 0.01-5 s^{-1} strain rate and constructed the constitutive equation (1) to describe the relationship between the flow stress, deformation temperature and strain rate. Furthermore, it has been calculated that the hot deformation activation energy of the alloy is 245.4 kJ /mol.

$$\dot{\varepsilon} = e^{28.47}[\sinh(0.013\sigma)]^{5.52} \exp\left(-\frac{245.4}{RT}\right) \quad (1)$$

In addition, after doping 0.03 wt.% P into the Cu-2Ni-0.5Si alloy under the same deformation conditions, Zhang *et al.* [56] studied the influence of P on the hot deformation activation energy of the alloy. The hot compression constitutive equation (2) of the alloy was constructed. It has been calculated that the thermal deformation activation energy of the Cu-2Ni-0.5Si-0.03P alloy was 485.6 kJ/mol.

$$\dot{\varepsilon} = 4.62 \times 10^{23}[\sinh(0.016\sigma)]^{7.06} \exp\left(-\frac{485.6}{RT}\right) \quad (2)$$

In order to investigate the influence of Ag on the hot deformation behavior of the Cu-Ni-Si alloy, Sun *et al.* [57] added 0.15 wt.% Ag into the Cu-2Ni-0.5Si alloy to prepare the Cu-2Ni-0.5Si-0.15Ag alloy and compared changes in the hot deformation process parameters of the two alloys. The results showed that the addition of Ag can refine grains and promote dynamic recrystallization. The hot deformation activation energy of the alloy after adding Ag was calculated to be 312.3 kJ/mol. Finally, the constitutive equation was constructed:

$$\dot{\varepsilon} = 8.67 \times 10^{11}[\sinh(0.018\sigma)]^{6.326} \exp\left(-\frac{312.3}{RT}\right) \quad (3)$$

2.3 Cu-Cr-Zr alloy

Cu-Cr-Zr alloy is widely used in high-speed rail contact lines and resistance electrodes due to its high strength and electrical conductivity [58–60]. Although Cu-Cr alloy has high conductivity, its strength is not outstanding. Adding a certain amount of Zr element to the Cu-Cr alloy can limit the coarsening of Cr precipitated phase during the aging process and further improve the alloy strength. Pan *et al.* [61] reported that Cu_5Zr nanoparticles precipitated out of the Cu-0.81Cr-0.12Zr alloy after aging and proposed that

Unauthenticated
Download Date | 12/11/19 7:47 AM

Table 1: The activation energy and constitutive equations of different alloys

Alloy	Q/(kJ/mol)	Constitutive equations
Cu-0.8Cr-0.3Zr	400.8	$\dot{\varepsilon} = e^{42.2}[\sinh(0.010\sigma)]^{9.11} \exp(-\frac{400.8}{RT})$
Cu-0.8Cr-0.3Zr-0.1Ag	343.23	$\dot{\varepsilon} = e^{35.82}[\sinh(0.011\sigma)]^{7.72} \exp(-\frac{343.23}{RT})$
Cu-0.8Cr-0.3Zr-0.05Nd	404.84	$\dot{\varepsilon} = e^{40.28}[\sinh(0.014\sigma)]^{7.19} \exp(-\frac{404.84}{RT})$

the best comprehensive properties could be obtained after aging for 15 min at 500°C: 212 HV microhardness and 78.9% IACS conductivity. While studying the effects of Zr and Mg on the precipitation and aging behavior of Cu-Cr alloy, Tang *et al.* [62] demonstrated that Zr-rich phase existed on the grain boundaries of the alloy, and the precipitated nano-phase hindered the movement of grain boundaries, thereby improving the fatigue and creep resistance of the alloy. Wang *et al.* [63] found that Zr-rich precipitated phases formed in the Cu-Cr-Zr alloy during the 450°C aging process. The habit plane of the two kinds of Zr-rich precipitated phases (Cu_4Zr and Cu_5Zr) were parallel to {111} Cu. Zhang *et al.* [64] studied the hot deformation behavior of the Cu-0.4Cr-0.1Zr alloy at 650-850°C and 0.001-10 s^{-1} strain rate, and calculated the activation energy for thermal deformation of the alloy at 392.48 kJ/mol. Consequentially, the hot deformation constitutive equation was constructed:

$$\dot{\varepsilon} = 4.929 \times 10^{16}[\sinh(0.017\sigma)]^{7.558} \exp\left(-\frac{392.48}{RT}\right) \quad (4)$$

In addition, the hot deformation behavior of the Cu-0.8Cr-0.3Zr, Cu-0.8Cr-0.3Zr-0.1Ag and Cu-0.8Cr-0.3Zr-0.05Nd alloys was studied [50]. The hot deformation activation energy and constitutive equations of these alloys are compared in Table 1.

According to the data analysis in Table 1, the addition of Ag effectively reduces the hot deformation activation energy of the Cu-Cr-Zr alloy, while the addition of Nd slightly increases the hot deformation activation energy of the alloy. This is because the grain refinement effect is more obvious after adding Ag.

3 Copper matrix composites

3.1 Hot deformation behavior of the copper matrix composites

Dispersion strengthened copper matrix composites have been widely used in the electronics industry as high voltage switches and resistance welding electrodes due to their excellent high-temperature strength, high electrical and thermal conductivity [65–68]. In general, nanoparticles, such as Al_2O_3, BeO, ZrO_2, Cr_2O_3, are usually employed as reinforcement in the dispersion strengthened copper matrix composites.

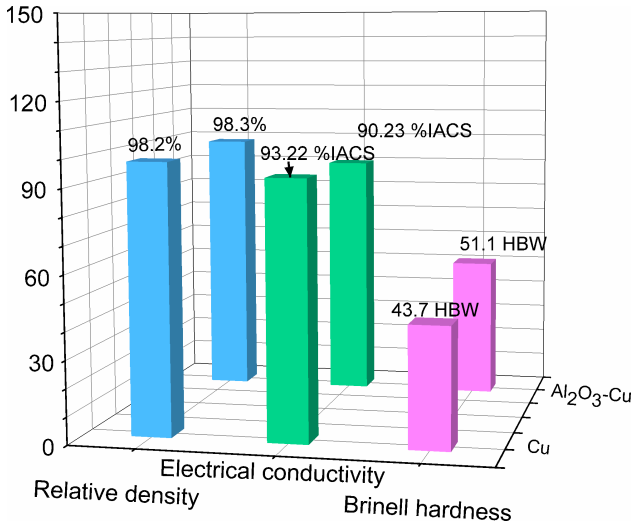

Figure 7: The comprehensive properties of pure copper and nano-Al_2O_3 reinforced composite. Label y axis.

Figure 7 shows the comprehensive properties of pure copper and nano-Al_2O_3 reinforced composite fabricated by the vacuum hot-pressing sintering and internal oxidation process. As shown in Figure 7, nano-Al_2O_3 phase in the copper matrix has a small negative effect on the electrical conductivity of the matrix. Tian *et al.* [69] prepared Cu-0.5vol.%Al_2O_3 by the internal oxidation method and reported that its softening temperature reached 800°C. Furthermore, it was demonstrated that the strengthening mechanism of the composite was not the Orowan bypass mechanism, but nano-alumina particles pinning grain boundaries and sub-grain boundaries to inhibit dynamic recrystallization. Mu *et al.* [70] used a powder metallurgy method to add Y_2O_3 into the copper matrix and studied its effect on the electrical contact material. Rodrigo *et al.* [71] prepared Cu-2vol.%TiC by using the ball milling method and studied its creep behavior to obtain its hot deformation activation energy of 109-156 kJ/mol. Yang *et al.* [72] fabricated Al_2O_3-Cu/10%TiC composite by vac-

Unauthenticated
Download Date | 12/11/19 7:47 AM

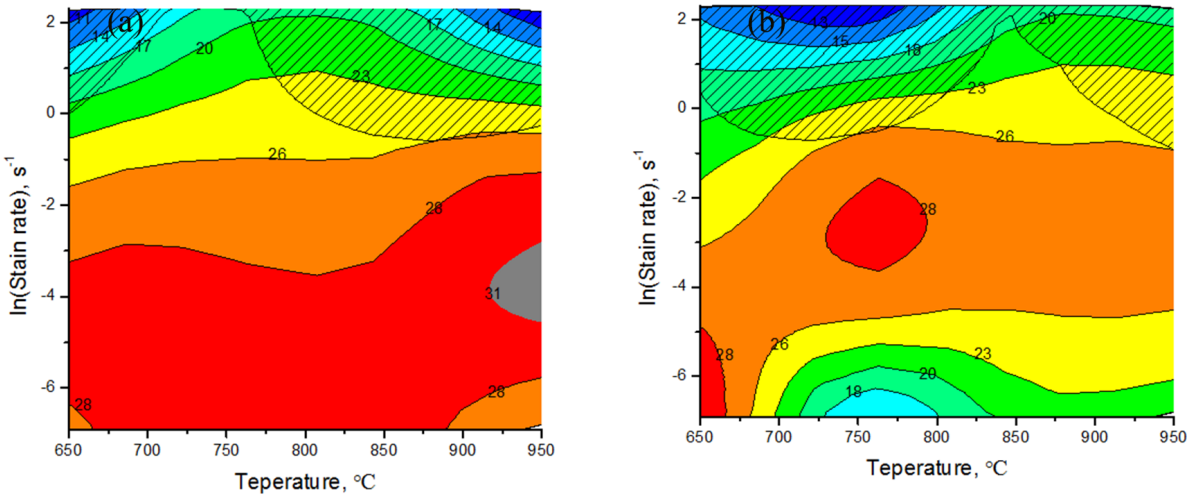

Figure 8: Hot processing maps of: (a) Al_2O_3-Cu/25W5Cr composite and (b) Al_2O_3-Cu/35W5Cr composite at 650-950°C.

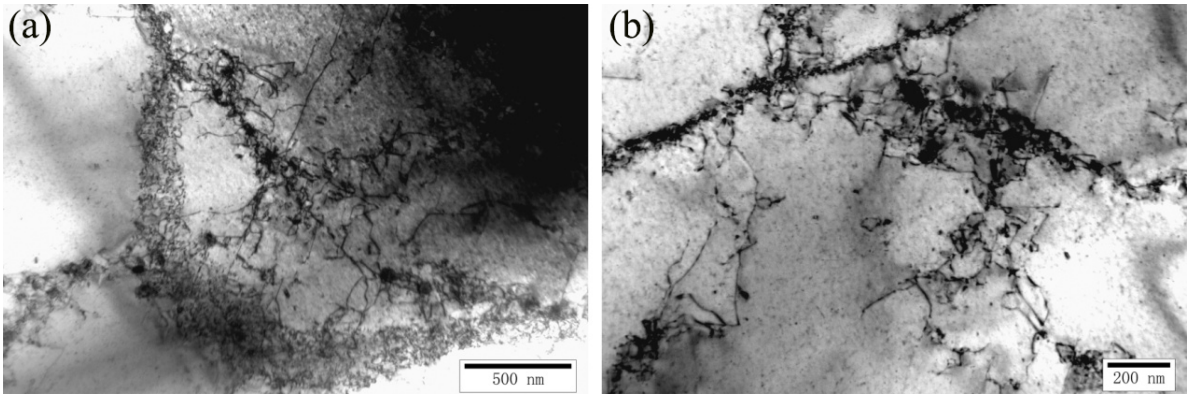

Figure 9: TEM images of the Al_2O_3-Cu/35W5Cr composite deformed at 850°C and 0.01 s^{-1}.

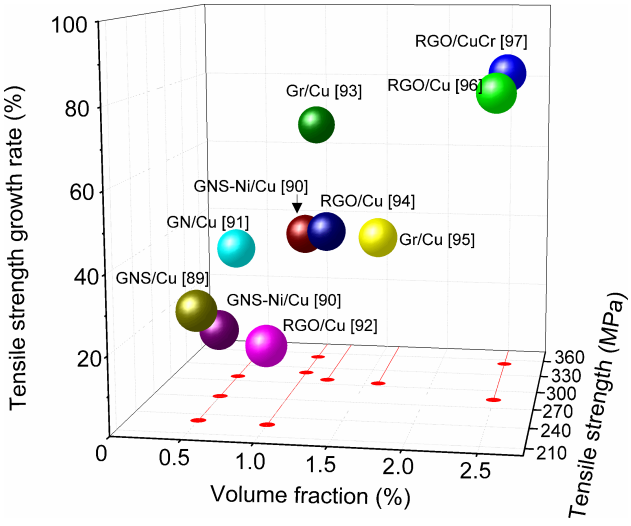

Figure 10: The tensile strength and tensile strength growth rate of the graphene reinforced copper matrix composites.

uum hot pressing sintering and internal oxidation method and studied its hot deformation behavior. The composite presented typical dynamic recrystallization characteristics in the process of hot deformation. It has been calculated that its hot deformation activation energy is 170.73 kJ/mol. Liu *et al.* [73] employed the same process to increase the TiC content to 20% and calculated the activation energy of 218.92 kJ/mol for the hot deformation process. By comparing the above research results, it can be demonstrated that the in-situ formation of Al_2O_3 or the increase of the nano-TiC particles amount can increase the activation energy of thermal deformation, thereby enhancing the deformation resistance of composites in the process of hot deformation. In order to improve the arc erosion resistance and circuit breaking ability of switch equipment, high melting point metals, such as W, Mo, Cr, etc. are often added to copper or dispersed copper matrix [74–77]. Hiraoka *et al.* [78] proposed that during compression of the W(80)/Cu composite grains became fibrous with larger deformation amount. Huang *et al.* [79] demonstrated that

Unauthenticated
Download Date | 12/11/19 7:47 AM

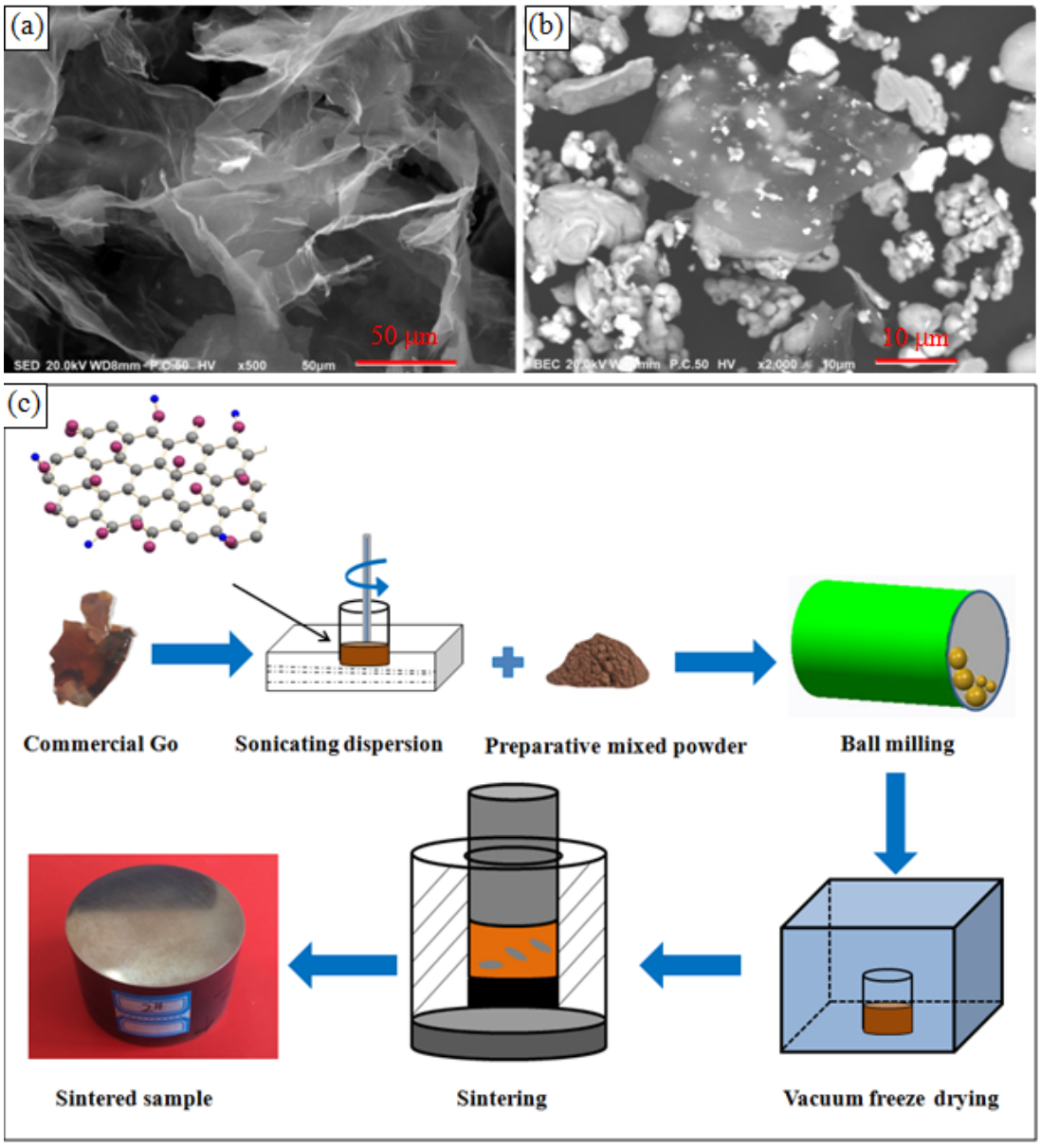

Figure 11: (a) The SEM image of the graphene oxide and (b) Composite powder doped with graphene oxide; (c) Schematics of the fabrication process.

the strengthening mechanism of the CuW70 alloy is work hardening caused by the sliding of the copper phase. Zou *et al.* [80] added a small amount of Cr and Ti to the Cu-W composite. These additions not only enhanced the interface bonding, but also improved the hot deformation performance of the composite. Zhang *et al.* [81] studied the thermal deformation behavior of the Al_2O_3-Cu/(W,Cr) composites, and the flow stress of the two kinds of composites increased rapidly to the maximum value and then gradually decreased to a steady value. Both kinds of composites show typical characteristics of dynamic recrystallization. In addition, at the same deformation temperature, the flow stress tends to increase with the strain rate and W content. In order to obtain the appropriate hot working conditions of the composites, hot processing maps were established in Figure 8. Furthermore, both stable and unstable regions were distinguished.

Finally, as shown in Figure 9, when the dislocations are pinned by nano-alumina particles, the dislocation wall changes from thick to thin. Under the deformation condition of 850°C and 0.01 s^{-1}, the copper matrix was still in the dynamic recovery stage.

Unauthenticated
Download Date | 12/11/19 7:47 AM

3.2 Graphene reinforced copper matrix composites

In recent years, graphene and its derivatives, such as graphene oxide (GO) and reduced graphene oxide (RGO) have attracted more attention as an ideal reinforcement of the metal matrix composites. Graphene is a 2D layered structure material with a thickness of a single-layer carbon sheet. Monolayer graphene has the Young's modulus of 1 TPa and the tensile strength of 130 GPa [82–86]. Therefore, graphene is considered as an ideal reinforcement for the development of high-performance metal matrix composites. At present, many researchers have prepared graphene reinforced copper matrix composites using powder metallurgy. Chu *et al.* [87] designed the graphene reinforced copper matrix composites by the vacuum filtration and spark plasma sintering methods. Compared with pure copper, the thermal conductivity of the composite increased by 50%. Varol *et al.* [88] reported that the highest conductivity was 78.5% IACS by adding 0.5 wt.% graphene into copper matrix composites. Figure 10 shows the tensile strength and tensile strength growth rate of the graphene reinforced copper matrix composites.

However, graphene has poor bonding with copper matrix and is prone to agglomeration in the preparation process. Fortunately, graphene oxide has large amounts of OH, COOH, C=O, and C(O)O groups. These groups are responsible for graphene oxide good wettability, dispersion and surface activity. In addition, they can enhance the bonding between the metal matrix and the reinforcement. Nevertheless, excellent conductivity can decrease sharply due to these groups. Actually, good conductivity can be obtained by reduction. For instance, one of the methods is heating at 900-1000°C, which greatly improves the conductivity due to the loss of oxygen-containing groups and the reconstruction of the carbon framework [98–100]. Ramirez *et al.* [101] reported that the GO can be reduced when GO/Si_3N_4 composites were sintered by the spark plasma sintering. Xia *et al.* [102] also proposed that GO could be reduced to RGO during high-temperature sintering.

Figure 11 shows the scanning electron microscopy (SEM) images of the graphene oxide and composite powder doped with graphene oxide. In our previous work, graphene oxide reinforced copper matrix composites were prepared by the freeze-drying and vacuum hot-press sintering methods, as shown in Figure 11(c). Furthermore, the tensile strength of the composite containing 0.3 wt.% GO was increased by 45%, as shown in Figure 12.

In the above studies, commercial GO or graphene as the ex-situ reinforcement phase of the metal matrix composites were prepared mostly by powder metallurgy. In situ reinforcement can improve the wettability and bonding at the graphene and metal interface through metallurgical reactions and chemical synthesis. Currently, many researchers use chemical vapor deposition (CVD) method to prepare graphene reinforced copper matrix composites [103–106]. Chen *et al.* [91] prepared 3D-GR/Cu composite with polymethyl methacrylate as carbon source, Cu as matrix and catalyst by using the CVD method. The tensile strength of the composite doped with 0.5 wt% was increased by 35.7%. Cao *et al.* [95] employed a bioinspired strategy by assembling copper flakes cladded with in situ graphene using polymethyl methacrylate as a solid carbon source. The yield strength and elastic modulus increased by 177% and 25%, respectively. Tour *et al.* [107] used a new solid carbon source to prepare graphene and doped graphene on the Cu surface, and the obtained graphene consisted of controllable layers and had low number of defects. In the previous work, the high growth temperature was required for graphene growth. However, Li *et al.* [108] used benzene as the hydrocarbon source to grow graphene in the CVD process, and the fabrication was achieved at a growth temperature as low as 300°C.

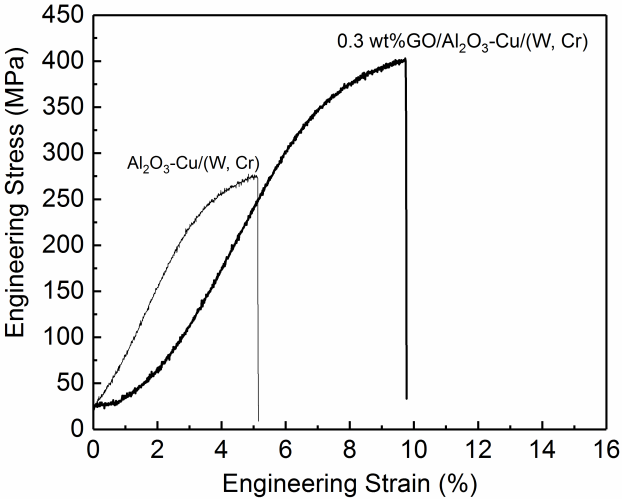

Figure 12: Engineering tensile stress-strain curves of different composites.

4 Conclusions

In this article, the aging precipitation and hot deformation behavior of several typical copper alloys have been reviewed. Nano-phase precipitated during aging can strengthen matrix owing to various strengthening mechanisms. Furthermore, hot deformation activation en-

Unauthenticated
Download Date | 12/11/19 7:47 AM

ergy and constitutive equation were calculated and constructed, respectively. In addition, nano-particles dispersion phase can strengthen copper matrix on the premise of ensuring electrical conductivity. Finally, graphene reinforced copper matrix composites were reviewed. CVD method is the most exceptional potential for fabricating graphene reinforced composites.

Acknowledgement: This work was supported by the Open Cooperation Project of Science and Technology of the Henan Province (182106000018), the Henan University Scientific and Technological Innovation Talent Support Program (18HASTIT024) and the National Natural Science Foundation of China (U1704143).

References

[1] Li R.G., Zhang S., Zou C.L., Kang H.J., Wang T.M., The roles of Hf element in optimizing strength, ductility and electrical conductivity of copper alloys, Mater. Sci. Eng. A, 2019, 758, 130-138.

[2] Ye Y.X., Yang X.Y., Wang J., Zhang X.K., Zhang Z.L., Sakai T., Enhanced strength and electrical conductivity of Cu–Zr–B alloy by double deformation–aging process, J. All. Compd., 2014, 615, 249-254.

[3] Liu J.B., Hou M.L., Yang H.Y., Xie H.B., Yang C., Zhang J.D., et al., In-situ TEM study of the dynamic interactions between dislocations and precipitates in a Cu-Cr-Zr alloy, J. All. Compd, 2018, 765, 560-568.

[4] Sun L.X., Tao N.R., Lu K., A high strength and high electrical conductivity bulk CuCrZr alloy with nanotwins, Scripta Materialia, 2015, 99 , 73-76.

[5] Khereddine A.Y., Larbi F.H., Azzedding H., Baudin T., Brisset F., Helbert A.L., et al., Microstructures and textures of a Cu–Ni–Si alloy processed by high-pressure torsion, J. All. Compd, 2013, 574 , 361-367.

[6] Zhang Z.J., Zhang P., Zhang Z.F., Cyclic softening behaviors of ultra-fine Grained Cu-Zn alloys, Acta Materialia, 2016, 121, 331-342.

[7] Wang B.J., Zhang Y., Tian B.H., An J.C., Volinsky A.A., Sun H.L., et al., Effects of Ce addition on the Cu-Mg-Fe alloy hot deformation behavior, Vacuum, 2018, 155, 594-603.

[8] Zou C.L., Chen Z.N., Guo E., Kang H.J., Fan G.H., Wei W., et al., A nano-micro dual-scale particulate-reinforced copper matrix composite with high strength, high electrical conductivity and superior wear resistance, RSC Adv., 2018, 8, 30777-30782.

[9] Han B.S., Guo E., Xue X., Zhao Z.Y., Li T.J., Xu Y.J., et al., Fabricating and strengthening the carbon nanotube/copper composite fibers with high strength and high electrical conductivity, Applied Surface Science, 2018, 441, 984-992.

[10] Wang H., Gong L.K., Liao J.F., Chen H.M., Xie W.B., Yang B., Restraining meta-stable fcc-Cr phase by restraining nucleation of equilibrium bcc-Cr phase in CuCrZrTi alloys during aging, J. All. Compd, 2018, 749, 140-145.

[11] Yang G., Li Z., Yuan Y., Lei Q., Microstructure, mechanical properties and e lectrical conductivity of Cu–0.3Mg–0.05Ce alloy processed by equal channel angular pressing and subsequent annealing, J. All. Compd, 2015, 640, 347-354.

[12] Xu C.Z., Wang Q.J., Zheng M.S., Zhu J.W., Li J.D., Huang M.Q., et al., Microstructure and properties of ultra-fine grain Cu–Cr alloy prepared by equal-channel angular pressing, Mater. Sci. Eng. A, 2007, 459, 303-308.

[13] Peng L.J., Mi X.J., Xie H.F., Yu Y., Huang G.J., Yang Z., et al., Microstructure and Properties of Cu-Cr-Zr-Ag Alloy, Mater. Sci. Forum, 2018, 941, 1613-1617.

[14] Zhang Y., Volinsky A.A., Tran Hai T., Chai Z., Liu P., Tian B.H., Effects of Ce addition on high temperature deformation behavior of Cu-Cr-Zr alloys, J. Mater. Eng. Perform., 2015, 24, 1-6.

[15] Tian K., Tian B.H., Zhang Y., Liu Y., Volinsky A. A., Aging strengthening mechanism of the Cu-1.0Zr alloy, Metall. Mater. Trans. A, 2017, 48A, 5628-5634.

[16] Wongsa J., Langdon T.G., Microstructural Evolution and Grain Refinement in a Cu-Zr Alloy Processed by High-Pressure Torsion, Mater. Sci. Forum, 2014, 783-786, 2635-2640.

[17] Wang W., Chen Z.N., Guo E.Y., Kang H.J., Liu Y., Zou C.L., et al., Influence of Cryorolling on the Precipitation of Cu–Ni–Si Alloys: An In Situ X-ray Diffraction Study, Acta Metall. Sinica, 2018, 31, 1089-1097.

[18] Wu Y.K., Li Y., Lu J.Y., Tan S., Jiang F., Sun J., Correlations between microstructures and properties of Cu-Ni-Si-Cr alloy, Mater. Sci. Eng. A, 2018, 731, 403-412.

[19] Ji G.L., Yang G., Li L., Li Q., Modeling constitutive relationship of Cu-0.4Mg alloy during hot deformation, J. Mater. Eng. Perform, 2014, 23, 1770-1779.

[20] Shukla A., Svs N.M., Sharma S.C., Mondal K., Constitutive modeling of hot deformation behavior of vacuum hot pressed Cu-8Cr-4Nb alloy, Mater. Design, 2015, 75, 57-64.

[21] Gao M.Q., Chen Z.N., Kang H.J., Li R.G., Wang W., Zou C.L., et al., Effects of Nb addition on the microstructures and mechanical properties of a precipitation hardening Cu-9Ni-6Sn alloy, Mater. Sci. Eng. A, 2018, 715, 340-347.

[22] Krishna S.C., Srinath J., Jha A.K., Pant B., Sharma S.C., George K.M., Microstructure and properties of a high-strength Cu-Ni-Si-Co-Zr alloy, J. Mater. Eng. Perform., 2013, 22, 2115-2120.

[23] Zhang Y., Tian B.H., Volinsky A. A., Sun H.L., Chai Z., Liu P., et al., Microstructure and precipitate's characterization of the Cu-Ni-Si-P alloy, J. Mater. Eng. Perform., 2016, 25, 1336-1341.

[24] Huang F.X., Ma J.S., Ning H.L., Geng Z.T., Lu C., Guo S.M., et al., Analysis of phases in a Cu-Cr-Zr alloy, Scripta Materialia, 2003, 48, 97-102.

[25] Cheng J.Y., Yu F.X., Ao X.W., Effect of trace yttrium on properties and micrestructure of Cu-0.6Cr-0.15Zr-0.05Mg-0.02Si alloy, Adv. Mater. Res., 2011, 239-242, 338-342.

[26] Tian K., Tian B.H., Zhang Y., Liu Y., Volinsky A.A., Aging strengthening mechanism of the Cu-1.0Zr alloy, Metall. Mater. Trans. A, 2017, 48A, 5628-5634.

[27] Dong Q.Y., Shen L.N., Cao F., Jia Y.L., Liao K.J., Wang M.P., Effect of t hermomechanical processing on the microstructure and properties of a Cu-Fe-P alloy, J. Mater. Eng. Perform., 2015, 24, 1531-1539.

[28] Wang B.J., Zhang Y., Tian B.H., Yakubov V., An J.C., Volinsky A.A., Liu Y., Song K.X., Li L.H., M. Fu, Effects of Ce and Y addition on microstructure evolution and precipitation of Cu-Mg alloy hot deformation, J. Alloy and Compounds, 2019, 781, 118-130.

[29] Zhang Y., Sun H.L., Volinsky A.A., Wang B.J., Tian B.H., Chai Z., Liu Y., Song K.X., Small Y addition effects on hot deformation

Unauthenticated
Download Date | 12/11/19 7:47 AM

behavior of copper-matrix alloys, Adv. Eng. Mater., 2017, 1700197, 1-10.
[30] Fang B.C., Li J.J., Zhao N.Q., Shi C.S., Ma L.Y., He C.N., et al., Boron doping effect on the interface interaction and mechanical properties of graphene reinforced copper matrix composite, Appl. Surf. Sci., 2017, 425 , 811-822.
[31] Livramento V., Marques M.T., Correia J.B., Almeida A., Vilar R., Preparation of Dispersion-Strengthened Coppers with Niobium Carbide and Niobium Boride by Mechanical Alloying, Mater. Sci. Forum, 2006, 514-516, 707-711.
[32] Chen B., Shen J., Ye X., Imai H., Umeda J., M. Takahashi, et al., Solid-state interfacial reaction and load transfer efficiency in carbon nanotubes (CNTs)-reinforced aluminum matrix composites, Carbon, 2017, 114, 198-208.
[33] Wang T.M., Zou C.L., Chen Z.N., Li M.Y., Wang W., Li R.G., et al., In situ synthesis of TiB_2 particulate reinforced copper matrix composite with a rotating magnetic field, Mater. Design, 2015, 65, 280-288.
[34] Long B.D., Othman R., Umemoto M., Zuhailawati H., Spark plasma sintering of mechanically alloyed in situ copper–niobium carbide composite, J. All. Compd, 2010, 505, 510-515.
[35] Xu Y.X., Sheng K.X., Li C., Shi G.Q., Self-assembled graphene hydrogel via a one-step hydrothermal process, ACS Nano, 2010, 4, 4323-4330.
[36] Bera S., Lojkowsky W.M., Development of wear-resistant Cu-10Cr-3Ag electrical contacts with alloying and high pressure sintering, Metall. Mater. Trans. A, 2009, 40, 3276-3283.
[37] Zhang X.H., Zhang Y., Tian B.H., Jia Y.L., Liu Y., Song K.X., et al., Thermal deformation behavior of the Al_2O_3-Cu/(W, Cr) electrical contacts, Vacuum, 2019, 164, 361-366.
[38] Xiao X.P., Xu H., Chen J.S., Liang Q.M., Wang J.F., Zhang J.B., Aging properties and precipitates analysis of Cu-2.3Fe-0.03P alloy by thermomechanical treatments, Mater. Res. Expr., 2017, 4, 116511.
[39] Wang W., Zou C.L., Li R.G., Wen W., Kang H.J., Wang T.M., In Situ Synchrotron X-Ray Diffraction Study of a Deformed Cu-Fe-P Alloy during Heating, Mater. Sci. Forum, 2016, 850, 191-196.
[40] Dong Q.Y., Shen L.N., Wang M.P., Jia Y.L., Li Z., Cao F., et al., Microstructure and properties of Cu–2.3Fe–0.03P alloy during thermomechanical treatments, Trans. Nonferr. Metals Soc. China, 2015, 25, 1551-1558.
[41] Guo F.A., Xiang C.J., Yang C.X., Cao X.M., Mu S.G., Tang Y.Q., Study of rare earth elements on the physical and mechanical properties of a Cu–Fe–P–Cr alloy, Mater. Sci. Eng. B, 2008, 147, 1-6.
[42] Cao H., Min J.Y., Wu S.D., Xian A.P., Shang J.K., Pinning of grain boundaries by second phase particles in equal-channel angularly pressed Cu–Fe–P alloy, Mater. Sci. Eng. A, 2006, 431, 86-91.
[43] Jia Y.L., Wang M.P., Chen C., Dong Q.Y., Wang S., Li Z., Orientation and diffraction patterns of δ-Ni_2Si precipitates in Cu–Ni–Si alloy, J. All. Compd., 2013, 557, 147-151.
[44] Wang W., Kang H.J., Chen Z.N., Chen Z.J., Zou C.L., Li R.G., et al., Effects of Cr and Zr additions on microstructure and properties of Cu-Ni-Si alloys, Mater. Sci. Eng. A, 2016, 673, 378-390.
[45] Hu T., Chen J.H., Liu J.Z., Liu Z.R., Wu C.L., The crystallographic and morphological evolution of the strengthening precipitates in Cu–Ni–Si alloys, Acta Materialia, 2013, 61, 1210-1219.
[46] Yi J., Jia Y.L., Zhao Y.Y., Xiao Z., He K.J., Wang Q., et al., Precipitation behavior of Cu-3.0Ni-0.72Si alloy, Acta Materialia, 2019, 166, 261-270.
[47] Xiao X.P., Yi Z.Y., Chen T.T., Liu R.Q., Wang H., Suppressing spinodal decomposition by adding Co into Cu-Ni-Si alloy, J. All. Compd, 2016, 660, 178-183.
[48] Zhao Z., Zhang Y., Tian B.H., Jia Y.L., Liu Y., Song K.X., Volinsky A.A., Co effects on Cu-Ni-Si alloys microstructure and physical properties, J. All. Compd, 2019, 797, 1327-1337.
[49] Lei Q., Xiao Z., Hu W.P., Derby B., Li Z., Phase transformation behaviors and properties of a high strength Cu-Ni-Si alloy, Mater. Sci. Eng. A, 2017, 697, 37-47.
[50] Zhang Y., An J.C., Jia Y.L., et al., Hot deformation and hot working process of copper matrix materials (in Chinese), Chem. Industry Press 2018 Beijing.
[51] Watanabe C., Nishijima F., Monzen R., Tazaki K., Mechanical Properties of Cu-4.0wt%Ni-0.95wt%Si Alloys with and without P and Cr Addition, Mater. Sci. Forum, 2007, 561-565, 2321-2324.
[52] Monzen R., Watanabe C., Microstructure and mechanical properties of Cu–Ni–Si alloys, J. Mater. Sci. Eng. A, 2008, 483-484, 117-119.
[53] Zhang Y., Tian B.H., Volinsky A.A., Sun H.L., Chai Z., Liu P., et al., Microstructure and Precipitate's Characterization of the Cu-Ni-Si-P Alloy, J. Mater. Eng. Perform., 2016, 25(4), 1336-1341.
[54] Li Z., Pan Z.Y., Zhao Y.Y., Xiao Z., Wang M.P., Microstructure and properties of high-conductivity, super-high-strength Cu–8.0Ni–1.8Si–0.6Sn–0.15Mg alloy, J. Mate. Res., 2009, 24, 2123-2129.
[55] Zhang Y., Tian B.H., Liu P., Jia S.G., Li F., Liu Y., Study on dynamic recrystallization behavior of Cu-Ni-Si alloy, Adv. Mater. Res., 2011, 146-147, 701-704.
[56] Zhang Y., Liu P., Tian B.H., Liu Y., Li R.Q., Xu Q.Q., Hot deformation behavior and processing map of Cu-Ni-Si-P alloy, Trans. Nonferr. Metals Soc. China, 2013, 23, 2341-2347.
[57] Sun H.L., Zhang Y., Volinsky A.A., Wang B.J., Tian B.H., Song K.X., et al., Effects of Ag addition on hot deformation behavior of Cu-Ni-Si alloys, Adv. Eng. Mater., 2017, 19, 1600607.
[58] Xia C.D., Zhang W., Kang Z.Y., Jia Y.L., Wu Y.F., Zhang R., et al., High strength and high electrical conductivity Cu–Cr system alloys manufactured by hot rolling–quenching process and thermomechanical treatments, Mater. Sci. Eng. A, 2012, 538, 295-301.
[59] Tian W., Bi L.M., Ma F.C., Du J.D., Effect of Zr on as-cast microstructure and properties of Cu-Cr alloy, Vacuum, 2018, 149, 238-247.
[60] Batawi E., Morris D.G., Morris M.A., Effect of small alloying additions on behaviour of rapidly solidified Cu-Cr alloys, Mater. Sci. Technol., 1990, 6, 892-899.
[61] Pan Z.Y., Chen J.B., Zhou W., Li J.F., Microstructure and properties of rapidly solidified Cu-0.81Cr-0.12Zr Alloy, Mater. Trans., 2013, 54, 1403-1407.
[62] Tang N.Y., Taplin D.M.R., Dunlop G.L., Precipitation and aging in high conductivity Cu-Cr alloys with additions of zirconium and magnesium, Mater. Sci.Technol., 1985, 1, 270-275.
[63] Wang K., Liu K.F., Zhang J.B., Microstructure and properties of aging Cu–Cr–Zr alloy, Rare Metals, 2014, 33, 134-138.
[64] Zhang Y., Sun H.L., Volinsky A.A., Tian B.H., Chai Z., Liu P., et al., Characterization of the hot deformation behavior of Cu-Cr-Zr alloy by processing maps, Acta Metall. Sinica, 2016, 29, 422-430.
[65] Han W.T., Chen D.S., Ha Y., Kimura A., Serizawa H., Fujii H., et al., Modifications of grain-boundary structure by friction stir welding in the joint of nano-structured oxide dispersion strengthened ferritic steel and reduced activation martensitic steel, Scripta Materialia, 2015, 105, 2-5.
[66] Chen F.Y., Ying J.M., Wang Y.F., Du S.Y., Liu Z.P., Huang Q., Effects of graphene content on the microstructure and properties of

Unauthenticated
Download Date | 12/11/19 7:47 AM

copper matrix composites, Carbon, 2016, 96, 836-842.
[67] Liu A.H., Ding H.Y., Zhou G.H., Zhang Y., Fretting tribology of Cu matrix composite reinforced by in situ Al_2O_3 particle, Adv. Mater. Res., 2011, 311-313, 26-31.
[68] Zhuo H., Tang J.C., Ye N., Strengthening mechanisms of Y_2O_3 dispersion strengthened copper-based composites, Rare Metal Mater. Eng., 2015, 44,1134-1138.
[69] Tian B.H., Liu P., Song K.X., Li Y., Liu Y., Ren F.Z., et al., Microstructure and properties at elevated temperature of a nano-Al_2O_3 particles dispersion-strengthened copper base composite, Mater. Sci. Eng. A, 2006, 435-436, 705-710.
[70] Zhen M., Geng H.R., Li M.M., Nie G.L., Leng J.F., Effects of Y_2O_3 on the property of copper based contact materials, Compos. Part B, 2013, 52, 51-55.
[71] Rodrigo H.P., Aquiles O.S., Creep behavior of two Cu-2 vol% TiC alloys obtained by r eaction milling and extrusion, Mater. Sci. Eng. A, 2013, 588, 82-85.
[72] Yang Z.Q., Liu Y., Tian B.H., Zhang Y., Model of critical strain for dynamic recrystallization in 10%TiC/Cu-Al_2O_3 composite, J. Centr. South Univ., 2014, 21, 4059-4065.
[73] Liu Y., Yang Z.Q., Tian B.H., Zhang Y., Gu Z.B., Volinsky A.A., Hot deformation behavior of the 20 vol.% TiC/Cu-Al_2O_3 composites, J. Mater. Eng. Perform., 2018, 27, 4791-4798.
[74] Zhang X.H., Zhang Y., Tian B.H., An J.C., Zhao Z., Volinsky A.A., et al., Arc erosion behavior of the Al_2O_3-Cu/(W, Cr) electrical contacts, Compos. Part B, 2019, 160, 115-122.
[75] Chang Y.L., Zheng W., Zhou Z.M., Zhai Y.X., Wang Y.P., Preparation and Performance of Cu-Cr Contact Materials for Vacuum Switches with Low Contact Pressure, J. Electr. Mater., 2016, 45, 5647-5654.
[76] Zhu S.X., Liu Y., Tian B.H., Zhang Y., Song K.X., Arc erosion behavior and mechanism of Cu/Cr20 electrical contact material, Vacuum, 2017, 143, 129-137.
[77] Li Q., Ding M., Wu A.P., Zou G.S., Song W., Li J., Anti-welding performance of copper-based electrical contacts in solenoid switch, Chin. J. Nonferr. Metals, 2013, 23(8), 2213-2220.
[78] Hiraoka Y., Hanado H., Inoue T., Deformation behavior at room temperature of W–80vol%Cu composite, Int. J. Refract. Metals & Hard Mater., 2004, 22, 87-93.
[79] Huang Y.T., Chen W.Z., Tang D.P., Study on microstructure and properties of CuW70 alloy under dynamic and static deformation, Heat Treatm. Metals, 2007, 32, 258-262.
[80] Zou J.T., Yang X.H., Liu G.F., Liang S.H., Deformability of Cu-W Composites with Addition of Cr, Ti Activated Elements, J. Comput. Theoret. Nanosci., 2011, 4, 1017-1021.
[81] Zhang X.H., Zhang Y., Tian B.H., Jia Y.L., Fu M., Liu Y., et al., Graphene oxide effects on the Al_2O_3-Cu/35W5Cr composite properties, J. Mater. Sci. Technol., 2019, (in press) DOI: 10.1016/j.jmst.2019.08.014.
[82] Kim J.Y., Lee W.H., Suk J.W., Potts J.R., Chou H., Kholmanov I.N., et al., Chlorination of reduced graphene oxide enhances the dielectric constant of reduced graphene oxide/polymer composites, Adv. Mater., 2013, 25, 2308-2313.
[83] Li N., Cao M.H., Hu C.W., Review on the latest design of graphene-based inorganic materials, Nanoscale, 2012, 4, 6205-6218.
[84] Zhu Y.W., Murali S., Cai W.W., Li X.S., Suk J.W., Potts J.R., et al., Graphene and graphene oxide: synthesis, properties, and applications, Adv. Mater., 2010, 22, 3906-3924.
[85] Tjong S.C., Recent progress in the development and properties of novel metal matrix nanocomposites reinforced with carbon nanotubes and graphene nanosheets, Mater. Sci. Eng. R, 2013, 74, 281-350.
[86] Lee C.G., Wei X.D., Kysar J.W., Hone J., Measurement of the elastic properties and intrinsic strength of monolayer graphene, Science, 2008, 321, 385-388.
[87] Chu K., Wang X.H., Wang F., Li Y.B., Huang D.J., Liu H., et al., Largely enhanced thermal conductivity of graphene/copper composites with highly aligned graphene network, Carbon, 2018, 127, 102-112.
[88] Varol T., Canakci A., Microstructure, electrical eonductivity and hardness of multilayer graphene/copper nanocomposites synthesized by flake powder metallurgy, Metals Mater. Int., 2015, 21, 704-712.
[89] Yue H.Y., Yao L.H., Gao X., Zhang S.L., Guo E., Zhang H., et al., Effect of ball-milling and graphene contents on the mechanical properties and fracture mechanisms of graphene nanosheets reinforced copper matrix composites, J. All. Compd, 2017, 691, 755-762.
[90] Tang Y.X., Yang X.M., Wang R.R., Li M.X., Enhancement of the mechanical properties of graphene–copper composites with graphene–nickel hybrids, Mater. Sci. Eng. A, 2014, 599, 247-254.
[91] Chen Y.K., Zhang X., Liu E., He C.N., Han Y.J., Li Q.Y., et al., Fabrication of three-dimensional graphene/Cu composite by in-situ CVD and its strengthening mechanism, J. All. Compd., 2016, 688, 69-76.
[92] Chu K., Wang J., Liu Y.P., Geng Z.R., Graphene defect engineering for optimizing the interface and mechanical properties of graphene/copper composites, Carbon, 2018, 140, 112-123.
[93] Li Z., Zhao L., Guo Q., Li Z.Q., Fan G.L., Guo C.P., et al., Enhanced dislocation obstruction in nanolaminated graphene/Cu composite as revealed by stress relaxation experiments, Scripta Materialia, 2017, 131, 67-71.
[94] Xiong D.B., Cao M., Guo Q., Tan Z.Q., Fan G.L., Li Z.Q., et al., Graphene-and-copper artificial nacre fabricated by a preform impregnation process: bioinspired strategy form strengthening-toughening of metal matrix composite, ACS Nano, 2015, 9, 6934-6943.
[95] Cao M., Xiong D.B., Tan Z.Q., Ji G., Ahmadi B.A., Guo Q., et al., Aligning graphene in bulk copper: Nacre-inspired nanolaminated architecture coupled with in-situ processing for enhanced mechanical properties and high electrical conductivity, Carbon, 2017, 117, 65-74.
[96] Hwang J., Yoon T., Jin S.H., Lee J., Kim T.S., Hong S.H., et al., Enhanced Mechanical Properties of Graphene/Copper Nanocomposites Using a Molecular-Level Mixing Process, Adv. Mater., 2013, 25, 6724-6729.
[97] Chu K., Wang F., Li Y.B., Wang X.H., Huang D.J., Zhang H., Interface structure and strengthening behavior of graphene/CuCr composites, Carbon, 2018, 133.
[98] Compton O.C., Nguyen S.T., Graphene Oxide, Highly reduced graphene oxide, and graphene: versatile building blocks for carbon-based materials, Small, 2010, 6, 711-723.
[99] Dimiev A.M., Tour J.M., Mechanism of graphene oxide formation, ACS Nano, 2014, 8, 3060-3068.
[100] Hu C.G., Zhai X.Q., Liu L.L., Zhao Y., Jiang L., Qu L.T., Spontaneous reduction and assembly of graphene oxide into three-dimensional graphene network on arbitrary conductive substrates, Sci. Rep., 2013, 3, 1-10.
[101] Ramirez C., Garzón L., Miranzo P., Osendi M.I., Ocal C., Electrical conductivity maps in graphene nanoplatelet/silicon nitride composites using conducting scanning force microscopy, Carbon,

Unauthenticated
Download Date | 12/11/19 7:47 AM

2011, 49, 3873-3880.
[102] Xia H.Y., Zhang X., Shi Z.Q., Zhao C.J., Li Y.F., Wang J.P., et al., Mechanical and thermal properties of reduced graphene oxide reinforced aluminum nitride ceramic composites, Mater. Sci. Eng. A, 2015, 639, 29-36.
[103] Cheng Y., Bi H., Che X.L., Li D.Z., Ji W.L., Huang F.Q., Suppression of graphene nucleation by plasma treatment of Cu foil for the rapid growth of large-size single-crystal graphene, Carbon, 2019, 147, 51-57.
[104] Eres G., Regmi M., Rouleau C.M., Chen J.H., Ivanov I.N., Puretzky A.A., et al., Cooperative island growth of large-area single-crystal graphene on copper using chemical vapor deposition, ACS Nano, 2014, 8, 5657-5669.
[105] Zhang Z.H., Xu X.Z., Qiu L., Wang S.X., Wu T.W., Ding F., et al., The way towards ultrafast growth of single-crystal graphene on copper, Adv. Sci., 2017, 4, 1700087.
[106] Kumar A., Voevodin A.A., Zemlyanov D., Zakharov D.N., Fisher T.S., Rapid synthesis of few-layer graphene over Cu foil, Carbon, 2012, 50, 1546-1553.
[107] Sun Z.Z., Yan Z., Yao J., Beitler E., Zhu Y., Tour J.M., Growth of graphene from solid carbon sources, Nature, 2010, 468, 549-552.
[108] Li Z.C., Wu P., Wang C.X., Fan X.D., Zhang W.H., Zhai X.F., et al., Low-temperature growth of graphene by chemical vapor deposition using solid and liquid carbon sources, ACS Nano, 2011, 5, 3385-3390.

Unauthenticated
Download Date | 12/11/19 7:47 AM